Journal of Non-Crystalline Solids 572 (2021) 121120

Contents lists available at ScienceDirect

Journal of Non-Crystalline Solids

journal homepage: www.elsevier.com/locate/jnoncrysol

Structural units of binary vanadate glasses by X-ray and neutron diffraction

U. Hoppe [a,*], A. Ghosh [b], S. Feller [c], A.C. Hannon [d], D.A. Keen [d], J. Neuefeind [e,1]

[a] Institut für Physik, Universität Rostock, 18051 Rostock, Germany
[b] Indian Association for the Cultivation of Science, School of Physical Sciences, Jadavpur, Kolkata 700032, India
[c] Coe College, Physics Department, Cedar Rapids, IA 52402, United States
[d] ISIS Facility, Rutherford Appleton Laboratory, Didcot OX11 0QX, United Kingdom
[e] DESY Photon Science, Notkestraße 85, 22607 Hamburg, Germany

ARTICLE INFO

Keywords:
Glass structure
X-ray diffraction
Neutron diffraction
Vanadate glasses
Second-order Jahn-Teller effects

ABSTRACT

X-ray diffraction with high-energy photons (synchrotron) and neutron diffraction are performed on binary vanadate glasses with MgO, Na_2O, K_2O to determine their structural units. The interpretation includes results of further binary vanadate glasses where vitreous V_2O_5 plays a key role. Different to the V_2O_5 crystal the structural model of the glass widely excludes three-fold coordinated oxygen according to Zachariasen's rules of glass formation. Results from the literature of an extensive analysis of vanadate crystals are used. VO_6 units exist in definite deformations. The corresponding out-of-center displacements of the V^{5+} ions are attributed to the second-order Jahn-Teller effects. The corresponding mechanisms are suggested to be effective also in glass structures. Two, three or four different V-O distances of this model are taken into account and allow a consistent modelling of the distributions of the bond lengths.

1. Introduction

The oxygen polyhedra of some glass-forming oxides show clear deviations from a regular shape. For example, strong distortions of the TeO_4 or TeO_3 units in tellurite glasses exist that are related to the effects of the non-bonding pair of electrons of the Te^{4+} ion [1]. The structural units of some other oxide glasses show distortions, as well, but the corresponding causes seem widely unclear. One of these systems is that of the vanadate glasses. The variations of their structural units and the corresponding distortions are the subject of this work. Vanadium oxides are candidates for rechargeable batteries [2]. Minor fractions of V^{4+} together with a majority of V^{5+} ions cause semi-conductivity due to polaron hopping [2]. Vanadium oxides are also interesting for applications in the catalysis [3].

The similarity of the stoichiometric formula of V_2O_5 with that of P_2O_5 may suggest a structural similarity with the phosphate glasses. High-energy X-ray diffraction (HEXRD) on vitreous (v-)V_2O_5 with high real-space resolution shows that bonds of different lengths exist in the VO_n units [4,5]. The shortest V-O bonds are related to the V=O double bonds. These are known of crystalline (c-)V_2O_5 where V=O bonds are directed to the apices of edge-connected VO_5 square pyramids [6]. Short P=O double bonds exist for v-P_2O_5 [7] and c-P_2O_5 [8], as well. The P=O bond occupies one of the corners of the PO_4 tetrahedron. PO_4 units are the only known structural units throughout all compositions of phosphate glasses. Here, is noted the arguments for the formation of the four-coordinated oxygen environments of the pentavalent phosphorus atoms. The ratio r_{cat}/r_{an} of the ionic radii (cation in the center) is used to assess the stability of definite polyhedral groups [9,10]. The optimum ratio r_{cat}/r_{an} for efficiently filling the space of a tetrahedron or octahedron is 0.225 or 0.414, respectively. The ratio for tetrahedral environment amounts to only 0.126 for the P^{5+} and O^{2-} ions whereby the radii given by Shannon & Prewitt [11,12] are used. Simply for these geometrical reasons, environments of the P^{5+} with more than four oxygen neighbors are very unlikely. The fifth valence of the P atom is attributed to a π-bond that shortens the P=O bond of the PO_4 [13]. The corresponding radius ratio for V^{5+} and O^{2-} ions is 0.263 for a VO_4 unit, which is a little larger than the optimum for a tetrahedron. The ratio is 0.400 for a VO_6 unit. That is almost ideal to form VO_6 octahedra and according to geometrical principles of dense packing, a regular VO_6 octahedron should be favored. Such VO_6 octahedra would be possible in the crystals c-V_2O_5 [6] or β-$VOPO_4$ [14] according to their network topology. However, the oxygens of some V-O-V bridges approach one of the two V neighbors to a short bond of ~ 0.157 nm, while the distance to the other side is elongated. In consideration of all these circumstances,

* Corresponding author.
E-mail address: uwe.hoppe@uni-rostock.de (U. Hoppe).
[1] Present address: Oak Ridge National Laboratory, P.O. Box 2008, Oak Ridge, TN 37831, USA

https://doi.org/10.1016/j.jnoncrysol.2021.121120
Received 11 May 2021; Received in revised form 3 August 2021; Accepted 12 August 2021
Available online 19 August 2021

the short V=O bonds must have different origin than the P=O bonds.

A possible underlying effect has been known for several decades. It is the spontaneous symmetry breaking of molecular systems according to the second-order Jahn-Teller (SOJT) effects [15–17]. Degeneracies of the electron levels of the molecular system induce the distortions. The d-orbitals of some transition metal ions Me^{k+} such as Ti^{4+}, V^{5+}, Cr^{6+}, Nb^{5+}, Mo^{6+} are empty. The energy gap between these empty d^0-orbitals of the Me^{k+} ion and the filled p-orbitals of the O^{2-} ligands of the MeO_6 is small. Their mixing results in nearly degenerate configurations and the elimination of the degeneracies produces the breakage of symmetry. For the MeO_6 octahedron that means an out-of-center distortion of the Me^{k+} ion as it exists in numerous crystal structures (Kunz & Brown [18]). The d^0-Me^{k+} ion leaves the center of the MeO_6 unit though it would fit this central position of MeO_6 geometrically very well.

The extent and direction of the out-of-center displacement of the Me^{k+} ions does not follow from the SOJT effects directly. The actual distortions depend on outer factors such as network restrictions, structural incommensurations, and second-neighbor repulsions [18]. One could argue that some Me^{k+} ions do not form MeO_6 octahedra but only MeO_5 pyramids or MeO_4 tetrahedra. However, the MeO_5 and MeO_4 units itself may result from strong SOJT distortions of the MeO_6 [18].

The analysis of SOJT effects for crystal structures is comparably simple [18]. The abundance and shape of the structural groups are directly accessible from the known three-dimensional structure. The step from knowing about SOJT effects of a transition metal ion such as V^{5+} to the understanding of the different VO_n polyhedra in the case of glasses is difficult. Diffraction methods on glasses yield only the distributions of pair distances. However, from knowing the detailed lengths, r_{VO}, of different V-O bonds and mean V-O coordination numbers, N_{VO}, one can deduce a reasonable overview of the structural units of the vanadate glasses. HEXRD is an excellent tool to determine N_{VO} and r_{VO} where the upper limit Q_{max} of the magnitude of scattering vector Q is the critical value of the resolving power. Values Q depend on the radiation wavelength λ and the scattering angle 2θ with $Q = (4\pi/\lambda)\sin\theta$. Neutron diffraction (ND) on spallation sources allows larger Q_{max} but the coherent scattering of neutrons on vanadium atoms is extremely weak. The combination of HEXRD and ND was often used in previous papers on vanadate glasses [4,5,19–22]. The change of contrast allows resolving the partial correlations of different atom pairs that contribute to the first-neighbor range. X-ray diffraction work of small Q-ranges exist [23–25] but such data are not included in our comparisons. Commonly, the Q_{max} of HEXRD is smaller than that available at neutron spallation sources. One cannot expect that excellent real-space resolution which was realized, for example, for the lengths of the two different P-O bonds in phosphate glasses [7,26,27]. A Q_{max} of 350 nm^{-1} allows resolving their difference with ~0.010 nm. Furthermore, variations of the distortions of the VO_n units could smear out the details of different V-O distances.

Diffraction results of some binary vanadate glasses modified with MgO, Na_2O, K_2O are presented in this work. The corresponding structural parameters will be used together with those of former work [4, 20–22] to analyze the compositional evolution of the oxygen polyhedra of the vanadate glasses. Comparisons with crystal structures will help to interpret the distance distributions of the V-O bonds.

2. Experimental

The samples of the series $(MgO)_x(V_2O_5)_{1-x}$ and $(A_2O)_x(V_2O_5)_{1-x}$ A=Na, K were prepared as described in [28] and [29], respectively. The Mg vanadate glasses were prepared from V_2O_5 and MgO. The melting temperatures were 750 °C to 1100 °C. The melts were quenched rapidly between two brass plates. The glasses were annealed at temperatures of 50 °C below the glass transition temperatures. Samples with thicknesses up to ~1 mm could be obtained. The mass densities of the samples were measured by the displacement method using acetone as the immersion liquid. In addition to the four samples of [28] (x = 0.1, 0.2, 0.3, 0.4), a glass with 50 mol% MgO was prepared. Its density was estimated by extrapolation. The alkali vanadate glasses were prepared from alkali carbonate and V_2O_5 by melting at ~850 °C in a platinum crucible. The molar ratios $R = (A_2O)/(V_2O_5)$ of the samples were 0.4, 0.6, 0.8 for A = K and 0.3, 0.6, 0.8, 1.2 for A = Na. The samples were obtained in glassy state by twin-roller quenching technique. Annealing was not possible. Densities were measured using the *Sink-Float* method or a helium pycnometer. Finally, the Mg vanadate samples of x = 0.2, 0.5 and the alkali vanadate glasses with R = 0.6 were used. Their sample labels are MgV20, MgV50, KV037 and NaV37.

The diffraction experiments (HEXRD and ND) were performed together with other series of the vanadate glasses. The alkali vanadate glasses were measured together with the Zn vanadate series [4] and the Mg vanadate glasses together with the Ca vanadate series [20]. HEXRD was performed at the BW5 beamline of the former synchrotron DORIS III of DESY Photon Science (Hamburg). The incident photon energy was 120.7 keV (radiation wavelength λ = 0.01027 nm) or 118.0 keV (λ = 0.01050 nm) for the alkali or magnesium glasses. The sample powders were loaded into thin-walled silica capillaries (diameters of 2.0 mm) and measured with a beam size of 1 × 4 mm^2. The scattering intensities were obtained in step-scan mode with a solid-state Ge-detector that was moved horizontally on a straight line. The intensities were obtained in several intervals of scattering angle with different absorbers to reduce the dead-time effects of the detector. Corrections were made for dead-time, background, container scattering, polarization, absorption, and varying sample-detector distance. The scattering intensities were normalized to structure-independent scattering functions which were obtained from a polynomial approach [30] of the tabulated atomic elastic scattering factors [31] and atomic Compton scattering data [32]. Finally, the Compton fraction is subtracted and the Faber–Ziman structure factors $S_X(Q)$ [33,34] are calculated from the normalized intensities.

The ND experiments were performed at the spallation source ISIS of the Rutherford Appleton Laboratory (Chilton/ UK) using the SANDALS or GEM instruments for the alkali or magnesium vanadate glasses, respectively. Only the two alkali vanadate samples of R = 0.6 that revealed free of obvious crystal fractions after HEXRD have been measured by neutrons. The powdered sample material was loaded into vanadium cylinders (diameter 5.0 mm, wall thickness 0.025 mm). The beam height was reduced to 10 mm due to the small amount of available sample material. According to the small angular range of SANDALS the Q-range is limited to 260 nm^{-1}. The Mg vanadate samples were measured on the GEM instrument that supplies a larger angular range of detector banks. The sample containers were the same vanadium cylinders and the beam size was reduced to 10 × 10 mm^2 due to limitations of sample material, as well. The data were corrected using standard procedures for container and background scattering, attenuation, multiple scattering and inelasticity effects by the ATLAS program suite [35]. The differential scattering cross-sections of the detector groups were used to compose the total neutron Faber–Ziman structure factors, $S_N(Q)$ [33, 34]. Before powdering the samples we tried to eliminate those flakes which were no longer transparent. This was not fully successful but the obvious crystal fractions of both alkali glasses and the 50 mol% Mg glass are very small and do not affect the structural analysis of the glasses.

3. Results

The final $S_N(Q)$ and $S_X(Q)$ structure factors are given in Fig. 1. The $S_N(Q)$ data are comparably noisy for Q > 200 nm^{-1} due to the lack of sufficient sample material. Fortunately, broad O-O, Mg-O and A-O distance peaks do not cause significant oscillations for larger Q-values. Even the O-O correlations of v-V_2O_5 [4] do not show oscillations for Q > 200 nm^{-1}. For the $S_X(Q)$ it is not clear if measuring ranges with Q_{max} > 250 nm^{-1} are really profitable. Such experiments would need much more measuring time in case of the step-scan mode used in the experiments.

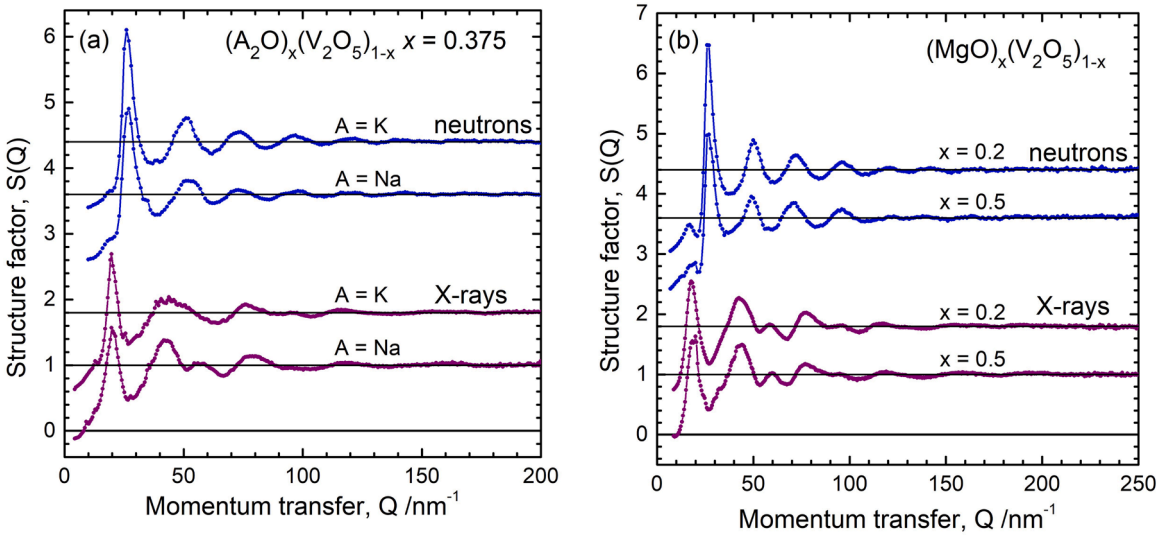

Fig. 1. Structure factors of the binary vanadate glasses obtained by ND (top) and HEXRD (bottom) experiments: (a) $(A_2O)_x(V_2O_5)_{1-x}$ with $x = 0.375$ and A = Na, K (b) $(MgO)_x(V_2O_5)_{1-x}$ with x = 0.2 and 0.5. The upper curves are shifted for clarity of the plot.

The correlation functions, $T_k(r)$, are obtained from the $S_k(Q)$ data by Fourier transform with

$$T_k(r) = 4\pi r\rho_0 + \frac{2}{\pi}\int_0^{Q_{max}} Q[S_k(Q) - 1]M(Q)\sin(Qr)dQ \quad (1)$$

The $T_k(r)$ functions of the four samples, where k means HEXRD or ND, are plotted in Figs. 2 and 3. The values Q_{max} are given in the figure captions, and also, if a damping function $M(Q)$, according to Lorch [36] is used. Damping reduces the effects of noise and unphysical features in the scattering range of large Q. The number densities, ρ_0, of atoms of samples KV037 and NaV37 are 62 and 69 nm^{-3} as calculated from the mass densities [29]. Values ρ_0 of 69 nm^{-3} are calculated for MgV20 and MgV50 samples from the mass densities in [28].

The T_X(r) functions show clear V-O first-neighbor peaks that will allow good determination of V-O coordination numbers. The V-O peaks of KV037, NaV37 and MgV20 are somewhat asymmetric with the weaker drop on their right flank. The combination with the neutron data is important in the case of MgV50 with an overlap of the V-O and Mg-O peaks. The first-neighbor peaks (r < 0.30 nm) are approximated with model functions that are composed of small series of Gaussian functions for the V-O, Na-O, Mg-O pairs. Single Gaussians are used for the K-O and O-O pairs. The parameters such as coordination numbers, mean distances and peak widths (full width at half maximum) are adjusted by means of least-square procedures. Termination effects of the Fourier transformations at Q_{max}, the effects of the damping function and of the Q-dependent X-ray weighting factors are simulated by convolution methods described in [25,37–39]. The resulting parameters are given in Table 1.

The asymmetric V-O peaks are well approximated with three Gaussians whereby the split in these three contributions is not free of arbitrariness. The total V-O coordination numbers decrease from 4.4 for MgV20 to 4.17 for MgV50 which follows the general trend from ~4.4 (v-V_2O_5 [4]) to ~4.0 at the metavanadate compositions (50 mol% metal

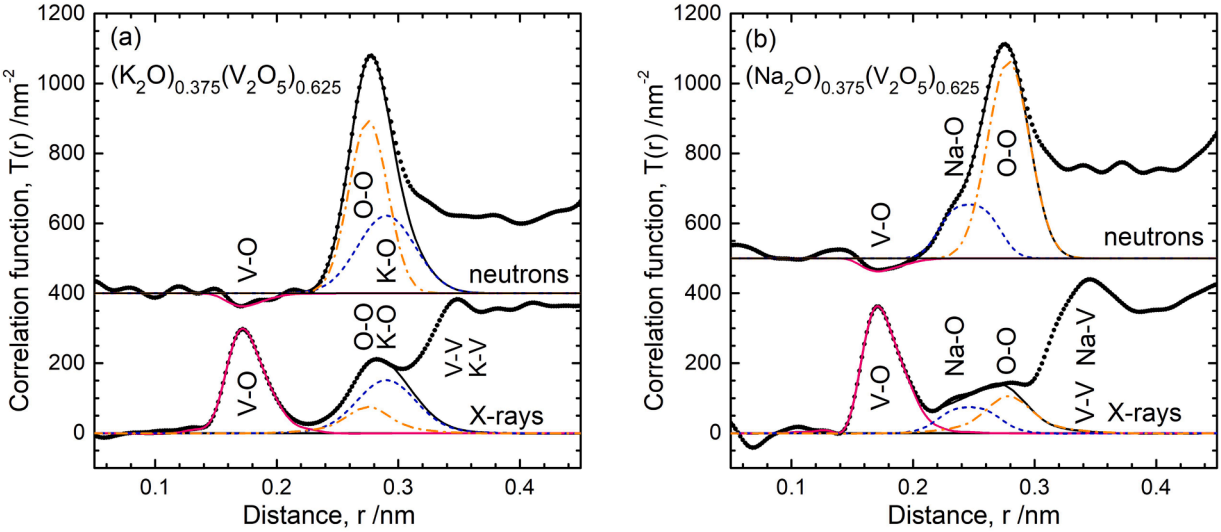

Fig. 2. Comparison of the total correlation functions, $T(r)$, of $(A_2O)_{0.375}(V_2O_5)_{0.625}$ glasses obtained from ND and HEXRD experiments (black dotted lines) with model functions in the range of the first-neighbor peaks (black solid lines): (a) A = K and (b) A = Na. The model partials are given as colored lines with V-O (solid – pink), A-O (dashed – blue), and O-O (dash-dotted – orange). The $T(r)$ are obtained with Q_{max} = 260 nm^{-1} (ND) and 260 nm^{-1} (HEXRD), both with damping according to Lorch [36]. The upper curves are shifted for clarity of the plot. (For interpretation of the references to color in this figure legend, the reader is referred to the web version of this article.)

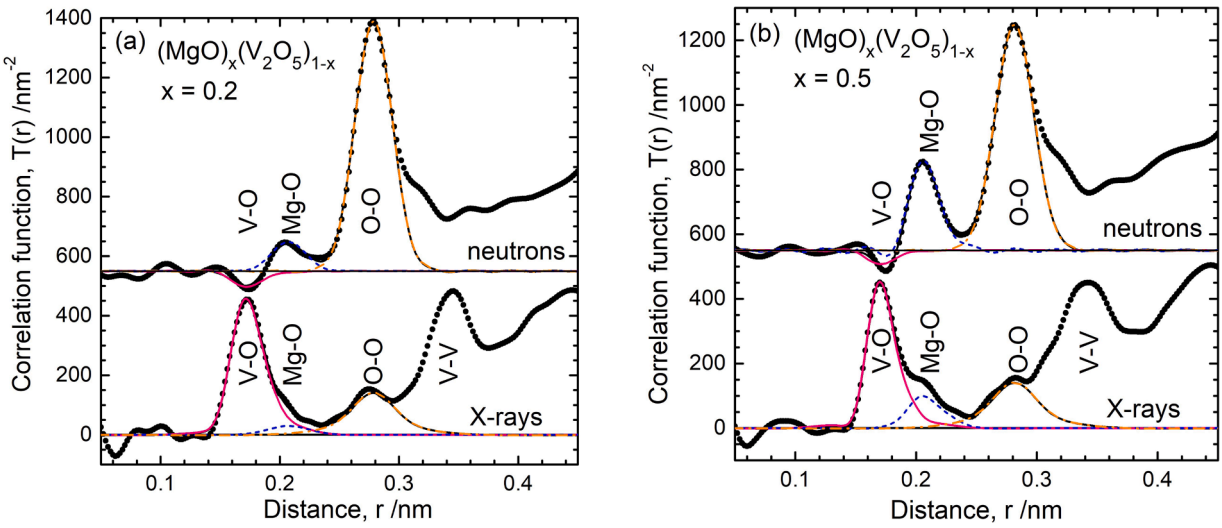

Fig. 3. Comparison of the total correlation functions, $T(r)$, of $(MgO)_x(V_2O_5)_{1-x}$ glasses obtained from ND and HEXRD experiments (black dotted lines) with model functions in the range of the first-neighbor peaks (black solid lines): (a) $x = 0.2$ and (b) $x = 0.5$. The model partials are given as colored lines with V-O (solid – pink), Mg-O (dashed – blue), and O-O (dash-dotted – orange). The $T(r)$ are obtained with $Q_{max} = 180$ nm^{-1} (ND) and 320 nm^{-1} (HEXRD), the latter with damping according to Lorch [36]. The upper curves are shifted for clarity of the plot. (For interpretation of the references to color in this figure legend, the reader is referred to the web version of this article.)

Table 1
Parameters of the Gaussian functions used for fitting the first-neighbor peaks of the $T_N(r)$ and $T_X(r)$ functions shown in Figs. 2 and 3. Parameters marked with asterisks were fixed in the fits. Since the different V-O, Mg-O and A-O Gaussian functions are not clearly resolved but only used to improve the fit, error bars are not given for the corresponding parameters. Distances and fwhm are given in nm (fwhm – full width at half maximum).

Sample label	Atom pair	Coordination number	Distance	fwhm	Total coordination number	Mean distance
KV037	V–O	1.75	0.167(2)	0.017(2)	4.17(15)	0.178(2)
		2.32	0.183(3)	0.028(3)		
		0.10	0.223(8)	0.028*		
	K–O	11.0	0.290(10)	0.053		
	O–O	4.24	0.275(5)	0.033(5)		
NaV37	V–O	1.55	0.165(2)	0.014(2)	4.23(15)	0.178(2)
		2.23	0.182(3)	0.026(3)		
		0.45	0.202(5)	0.026*		
	Na–O	2.7	0.233	0.026	5.9(3)	0.248(4)
		3.2	0.259	0.027		
	O–O	5.3(3)	0.279(5)	0.037(5)		
MgV20	V–O	2.40	0.168(2)	0.021(2)	4.40(15)	0.177(2)
		1.73	0.183(3)	0.030(3)		
		0.27	0.209*	0.030*		
	Mg–O	4.3	0.207(3)	0.022(4)	6.0(4)	0.208(4)
		1.7	0.209*	0.030*		
	O–O	6.6(5)	0.279(5)	0.036(4)		
MgV50	V–O	2.57	0.168(2)	0.017(2)	4.17(15)	0.175(2)
		1.54	0.183(3)	0.026(3)		
		0.06	0.220*	0.025*		
	Mg–O	3.18	0.203(2)	0.019(3)	4.88(20)	0.209(3)
		1.70	0.220*	0.025*		
	O–O	6.7(5)	0.282(5)	0.038(4)		

oxide) [20]. All N_{VO} results used in the Discussion chapter follow this behavior. An uncertainty of ±0.1 for N_{VO} must be taken into account. Oxygen coordination numbers of five to six are reasonable values for the Mg^{2+} and Na^+ ions. The oxygen coordination number of 11.0 for K^+ is too large. The separation of the K-O and O-O coordination numbers was unsuccessful with too large N_{KO} and too small N_{OO} values. To solve the problem one would have to include distances of the V-O second neighbors or to fix the K-O distances according to known crystal data.

4. Discussion

4.1. Distributions of the lengths of V–O bonds

Vanadium oxides exist in large varieties of structural units with VO_4, VO_5 and VO_6 polyhedra, each of them with different conformations and connectivities [40]. A long list of spectral parameters allows classifying these structures by ^{51}V NMR techniques. On the other hand, NMR studies of vanadate glasses are rare. A ^{51}V NMR study of glasses $(MO)_x(V_2O_5)_{1-x}$ for $0.30 \le x \le 0.55$ and M = Ca, Sr, Ba [41] reported VO_4 tetrahedral groups of different connectivities. A similarity with phosphate networks was suggested [41]. However, the total V-O coordination numbers from the diffraction methods are not constant four but show a significant decrease with modifier additions from ~4.4 to ~4.0. Some VO_5 or VO_6 groups must exist in the glasses of small modifier content.

The diffraction measurements with large Q_{max} yield a good real-space resolution with regard to the bond lengths. The broadening of the peaks caused by the upper limit of the Fourier transforms (cf. Eq. (1))

is small. It is therefore worthwhile to analyze the distance distributions more closely. Fig. 4 shows the comparisons of numerous V-O model peaks. The length distributions are calculated with the present (Table 1) and reported parameters of Gaussian functions. The results are arranged in groups of similar content of metal oxide (MO or M_2O). The model distributions are free of any broadening that would arise from the termination with Q_{max} and the use of damping in the Fourier transforms. The model peaks are compared free of experimental influences such as the different scattering weight of the V-O pairs.

The areas of the peaks in Fig. 4 are directly related to the numbers of atomic neighbors as usual for the radial distribution functions $RDF(r)$. This function is obtained from the correlation function $T(r)$ by $RDF(r) = r \cdot T(r)$. It is common to perform the fits with Gaussian peaks to the $T(r)$ functions [38,39]. In this case, the Gaussian peaks correspond to damped sinusoidal contributions in the interference functions $i(Q) = S(Q) - 1$. The Gaussian functions that are calculated with the parameters from Table 1 are multiplied with distance r and renormalized by a factor before added to the curves in Fig. 4.

4.2. Vitreous V_2O_5 and V_2O_5-P_2O_5 glasses

Fig. 4(a) starts with some remarkable V-O distances that were obtained for the V_2O_5-P_2O_5 glasses [21] and v-V_2O_5 [4]. Recent HEXRD data of such glasses report V-O coordination numbers of 4.43 for v-V_2O_5 and a subtle increase of N_{VO} with P_2O_5 additions [5], which agrees with our findings [21]. Unfortunately, significant V^{4+} fractions are inevitable if P_2O_5 is added to V_2O_5 and this effect depends on the conditions of the sample preparation. Large fractions V^{4+}/V of 0.57 were analyzed for a glass with 44 mol% P_2O_5 [5] and 0.35 for a glass with 50 mol% P_2O_5 [21].

At present, the interactions of the V^{5+} and V^{4+} sites in the glasses are not understood. Surprisingly, the crystals β-$VOPO_4$ with V^{5+} [42] and $(VO)_2P_2O_7$ with V^{4+} [43] form similarly distorted VO_6 units, each with a short V-O bond (0.156 nm and 0.160 nm). The appropriate mixture of the V-O distances of these crystals agrees excellently with the bond lengths of the $(V_2O_{4.65})_{0.5}$-$(P_2O_5)_{0.5}$ glass [21]. An EXAFS work [44] reported that the variations of the V^{4+}/V ratio of V_2O_5-P_2O_5 glasses change the signal only marginally. Thus, V^{5+} and V^{4+} ions have similar oxygen environments in those crystals [42,43] and in the corresponding glasses. The distorted VO_6 units of the crystals and glasses are interpreted as VO_5 square pyramids. The peak of the short V=O bond is separate from all V-O bonds to the base of the pyramid (Fig. 4a top). The latter bonds form V-O-P bridges (β-$VOPO_4$ [42]), which is adopted for the corresponding glass, as well. With decreasing P_2O_5 content, the V-O-V bridges between VO_5 pyramids cannot simply replace these V-O-P bridges. Three corners of the pyramidal base of the VO_5 units of c-V_2O_5 [6] have three-fold coordinated O atoms. The neighboring pyramids are connected via edges. Presumably, these constraints prevent forming equivalent networks in the V_2O_5 glass. Three-fold coordinated oxygens and edge-connected units are not suited as building principle for glass formation according to Zachariasen's rules [45]. The value N_{VO} of v-V_2O_5 is only ~4.5 [5,21] but not five as for c-V_2O_5 [6]. The peak of short V=O bonds of v-V_2O_5 (Fig. 4a) shifts to a little larger distance if compared with that of the V_2O_5-P_2O_5 glasses. Hence, not all of the structural units of vitreous V_2O_5 can own a terminal V=O double bond. A plausible description of the structure of vitreous V_2O_5 is still unknown. An even smaller V-O coordination number of only 3.9 was obtained for molten V_2O_5 [46]. The resolving power of that diffraction experiment was small. The short V=O distances were not detected separately.

4.3. Additions of modifier oxide

The changes of the V-O bonds with the additions of metal oxides are illustrated in Fig. 4 beginning with v-V_2O_5 in Fig. 4a. Three to seven distributions for each of the four intervals of compositions are shown in Fig. 4b. The curves of an interval are very similar each other. The data of the measurements of this work are given as dashed lines. The data of the MgV20 and MgV50 samples fit the older data very well. The V-O lengths of the NaV37 and KV037 samples show two peak components and are a little broader than those of the glasses modified with MO. The distributions of V-O bonds seem not to change smoothly from v-V_2O_5 to the metavanadate glasses (50 mol% MO). The character with three peak components as for v-V_2O_5 is still visible for the 10 mol% SrO glass but it is lost for the 20 mol% glasses. Starting from that point, the distributions change smoothly. Mean values of several parameters are indicated in Fig. 4. The N_{VO}'s decrease to finally four at metavanadate composition, which is accompanied by a just significant shortening of the mean distances r_{VO}. The more obvious change is a continuous narrowing of the

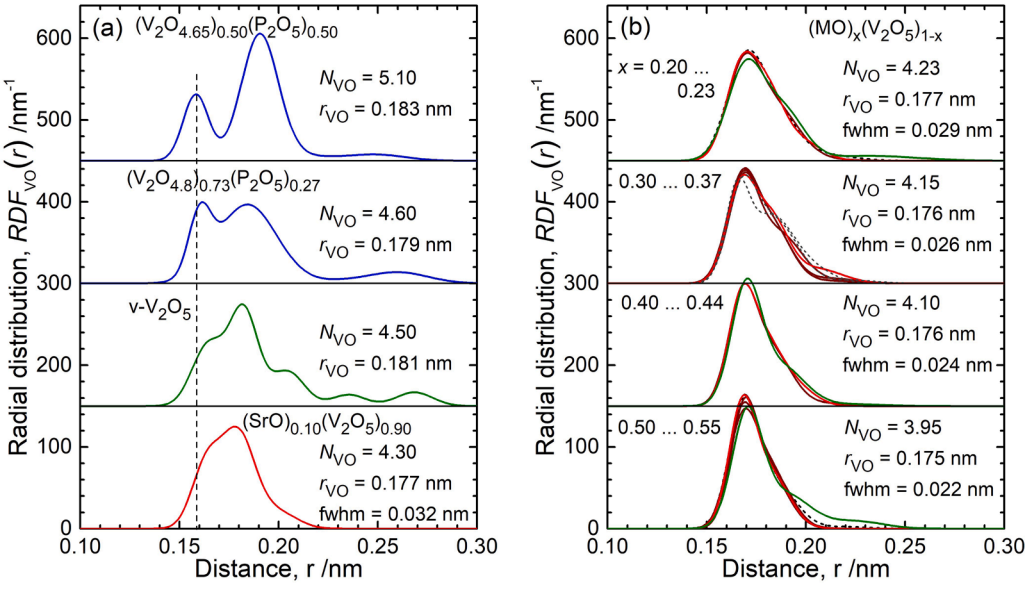

Fig. 4. Evolution of the V-O first-neighbor distances of numerous binary vanadate glasses by means of their radial distributions. The peaks are arranged in groups according to the glass compositions. The curves are calculated with the fit parameters as given for: (a) two vanadium-phosphate glasses and v-V_2O_5 [21], $(SrO)_{0.10}(V_2O_5)_{0.90}$ glass [22] and (b) vanadate glasses with about 20, 30, 40 and 50 mol% modifier oxide (green solid lines – M = Zn [4], red solid lines – M = Sr [22], brown solid lines – M = Ca [20], dashed lines - this work). The coordination numbers, N_{VO}, mean distances, r_{VO}, and full widths at half maximum (fwhm) are given. In part (b), these values are mean numbers of all samples. The tails of r_{VO} > 0.22 nm are not included in the calculations. The vertical dashed line in part (a) indicates the length of the terminal V=O bond. The upper curves are shifted for clarity of the plot. (For interpretation of the references to color in this figure legend, the reader is referred to the web version of this article.)

distributions with fwhm values of 0.032 nm for 10 mol% to 0.022 nm for 50 mol% MO. The evolution of the P-O distances of modified phosphate glasses shows partial similarities beginning with a small peak of P=O bonds and a three-times larger peak of single P-O bonds for v-P_2O_5 [7]. Except for the isolated PO_4 of orthophosphate glasses with a single peak one finds always two distance peaks, both with equal fractions at metaphosphate compositions [27].

Many crystal structures are known for the $(MO)_x(V_2O_5)_{1-x}$ systems but all of them with $0.5 \leq x$. VO_5 square pyramids exist in the structures of $x = 0.5$ for M = Zn, Mg, Ca, Sr [47-50] while N_{VO} values close to four are found for the corresponding metavanadate glasses. That suggests VO_4 tetrahedra connected via two corners such as proposed by ^{51}V NMR [41]. VO_4 units are known of the $NaVO_3$ [51] and KVO_3 [52] crystal structures ($x = 0.5$) with two V-O bonds of 0.164 nm to the terminal sites and two bonds of 0.180 nm in V-O-V bridges. If the lengths would be changed to 0.167 nm and 0.178 nm that would allow an excellent fit with two peaks of equal area in case of sample MgV50. One can assume the lengths of MgV50 to represent bond valencies of 1.5 and 1.0 of the V-O bonds where Mg^{2+} ions interact only with the terminal O sites. Close interaction of the alkali ions with the O in the V-O-V bridges elongates (weakens) the bridging bonds while the terminal V-O bonds are shortened (strengthened). That explains the differences to the bond lengths of the alkali MVO_3 crystals. The N_{VO} of sample MgV50 is a little larger than four and a few V-O bonds of lengths $r_{VO} > 0.19$ nm exist. This fraction is attributed to few VO_5 units of unknown conformation.

The two alkali vanadate samples NaV37 and KV037 possess compositions of 37.5 mol% M_2O. For a structure of corner-connected VO_4 units similar to that of phosphate glasses a numeral ratio of terminal to bridging V-O bonds of 0.67 is expected. Thus, fractions of 1.6 and 2.4 should result for the short and long V-O bonds, respectively. These values agree with the results in Table 1 with bond lengths of ~0.166 nm and ~0.182 nm. This is a surprising success. The V-O peaks in Fig. 2 are broad without any visible split. Obviously, the characteristic asymmetries of these peaks have influenced the fit. The small excess of $N_{VO} > 4.0$ and few longer distances $r_{VO} > 0.19$ nm are attributed to few VO_5 units of unknown conformation. For comparisons, the structure of the LiV_3O_8 crystal [53] is considered. Its composition is equivalent to a glass of 33 mol% M_2O. Three different V sites exist which form distorted VO_6 units. Two of them can be interpreted as VO_5 square pyramids, one VO_6 shows another distortion.

4.4. Simple structural model

Assuming the model of phosphate glasses for the MgV20 sample ($N_{VO} = 4.3$) that should give a numeral ratio of short and long V-O bonds of 0.45. The numbers in Table 1 yield a ratio of 1.4. It is not possible to obtain reasonable V-O distances together with that ratio of 0.45. Thus, the vanadate glasses require another model. In a first step, we focus on the structure of vitreous V_2O_5. In previous work with results on v-V_2O_5 [4,5,54,55] a V-O coordination number of ~4.5 is obtained. The atomic configurations from reverse Monte-Carlo (RMC) [55] show a special dilemma. The V-O peak is well reproduced by the simulations. As expected for v-V_2O_5, most O atoms form V-O-V bridges while a small part forms terminal V=O bonds. The mixture of VO_4 and VO_5 units of various conformations satisfies N_{VO} = ~4.5. The given constraints are average parameters that are effective only throughout all structural units. The RMC work [55] does not take account of the individualities of the units. No one constraint in RMC will prevent long terminal V-O bonds or V-O-V bridges with two short bonds. The bond lengths correlate with the valences of the bonds according to the bond valence model [56]. The sum rule of bond valences demands the sum of valences of the bonds of an atom to equal the valence of this atom [56]. Thus, the large variety of shapes of the VO_n polyhedra from RMC is rather not real but owed to the randomness in the algorithm. Probably, less diversity of groups exists. One might improve the method of structural simulation and try to construct a V_2O_5 model that takes into account the bond valences. Here we suggest to consider the detailed V-O distances from HEXRD and to use the knowledge of the structures of the vanadate crystals.

The fit of the V-O distances of v-V_2O_5 [21] (Fig. 4a) yielded 1.5 neighbors at 0.164 nm, 2.1 at 0.182 nm, 0.9 at 0.204 nm and few longer distances. The different V-O distances can be attributed to definite bond valences on the basis of selected crystal structures (Table 2). The approximation of Brown & Altermatt [58] yields very similar results. Thus, the large maximum at ~0.180 nm represents the single V-O bonds. The short bonds include a fraction of terminal V=O double bonds. Other short bonds participate in V-O-V bridges and, therefore, must be balanced with the longer bonds.

An extensive analyses of numerous vanadate crystals has already been carried out [59] namely with regard to the second-order Jahn--Teller (SOJT) effects (cf. Introduction) [18,60]. The variety of possible VO_6, VO_5 and VO_4 units reduces according to this consideration. Regular VO_6 do not exist. Regular VO_4 units are known of orthovanadate crystals such as Li_3VO_4 [57] but are not expected for v-V_2O_5. These isolated VO_4 are formed due to the lack of oxygens and a large volume fraction of the modifier ions which require large interstices in the case of orthovanadates. Common characteristics of the VO_n oxygen environments are the distortions that are attributed to the SOJT effects [18,59,60]. The starting point is the MeO_6 octahedron where the transition metal ion Me^{k+} must leave the central position. Three out-of-center displacements of the transition metal ions Me^{k+} with empty d^0-orbitals are known [18, 60] (cf. Fig. 5) that are observed for the different Me^{k+} in characteristic ways.

Here, the specifics given in [59] for the V^{5+} ion are summarized: V^{5+} ions are classified as strong distorters. Large out-of-center displacements of ~0.040 nm of the V^{5+} ions exist (mean value). The direction of displacement is mostly a corner of the VO_6 octahedron, which results in VO_5 square pyramids with one short bond. Another fraction shows displacements to an edge. This can result in distorted VO_4 tetrahedra with two short and two medium bonds while the two O sites of the longer bonds may be too far to be registered. Displacements to faces do not play any role for the V^{5+} ions. A few crystal structures show intermediate forms of distortions. Regular VO_6 do not exist. The authors [59] have also analyzed if the oxygens of the VO_6 resist in their octahedral positions after the out-of-center displacements of the V^{5+}. The main effect is the displacement of the V^{5+} ion while the oxygen positions appear less shifted.

The consideration of the VO_6 distortions is helpful because three to four different V-O distances must co-exist in the various VO_n units of v-V_2O_5 (cf. Fig. 5). A VO_5 has one short and four long V-O bonds. The VO_4 unit has two short and two long V-O bonds. The possible remaining V-O distances of the VO_6 are much longer ($r_{VO} > 0.22$ nm) and contribute only little bond valence. From the influence of the SOJT effects we suggest characteristic units for v-V_2O_5. That is a VO_5 square pyramid with a short V=O double bond (0.158 nm), two single bonds of 0.182 nm and two weaker bonds (bond valence 0.5) of 0.203 nm. The VO_4 has two short bonds of 0.167 nm (bond valence 1.5) and two single bonds of 0.182 nm. Both units exist in equal fractions. One can construct a network with these VO_5 and VO_4 forming linkages that are balanced concerning their valencies (cf. Fig. 6). The bridges with bond valencies

Table 2
Lengths of V-O bonds in dependence on their bond valence. The given lengths belong to linkages of appropriate bond valence in definite crystal structures. The length to bond valence 1.5 is taken from the short bond of the MgV50 metavanadate glass. For bond valence 0.5 only a rough estimation is possible.

Bond valence	Bond length (in nm)	Crystal structure
2.0	0.156	β-$VOPO_4$ [14]
1.5	0.167	estimated
1.25	0.172	Li_3VO_4 [57]
1.0	0.178	c-V_2O_5 [6]
0.75	0.189	β-$VOPO_4$ [14]
0.5	0.203	estimated

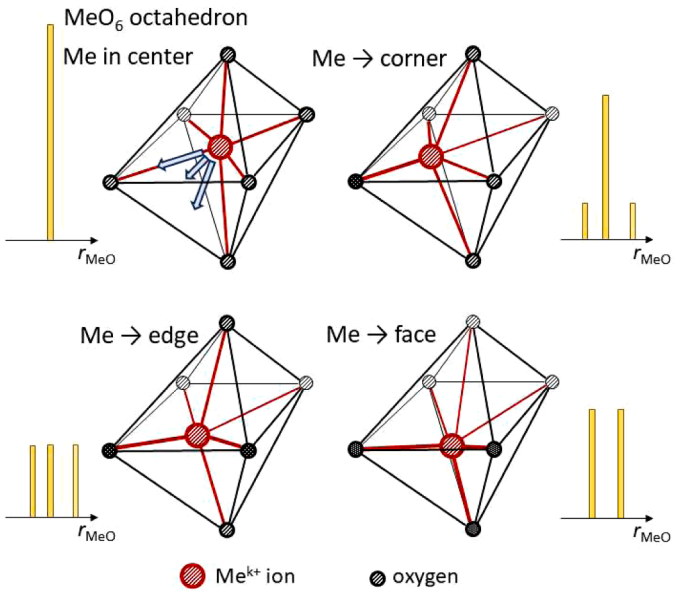

Fig. 5. Out-of-center distortions of the V atoms in octahedral oxygen environments according to the SOJT effect [15–18]. The typical directions of distortion are indicated in the left-upper octahedron by three arrows. The corresponding distortions are shown in the other three octahedra. The resulting distributions of bond lengths (V-O) of each octahedron are indicated by bar graphs.

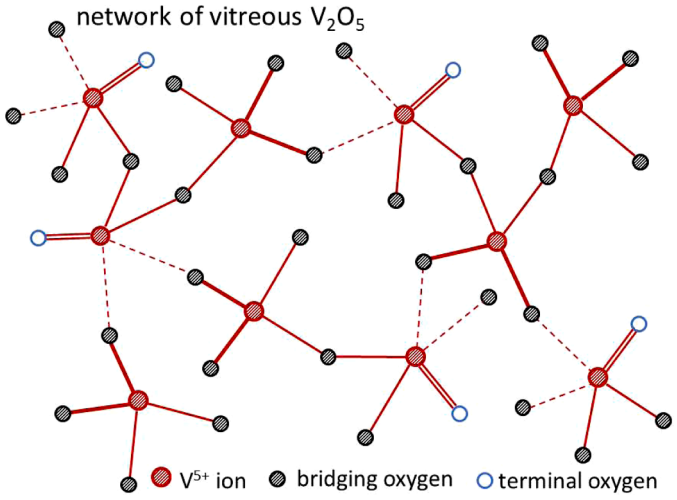

Fig. 6. Section of the network model for the vitreous V_2O_5. V-O bonds of different valencies are identified by their line width or line type: V=O – double line; bond valence 1.5 – thick solid line; single bond – thin solid line; bond valence 0.5 – thin dashed line.

1.5 and 0.5 connect a VO_4 with a VO_5 unit while the bridges with single bonds can connect any like or unlike groups. This flexibility of linkages guaranties that the units can form a disordered network. Fig. 7 shows a good fit of these V-O distances with the appropriate abundances of different bonds to the bond length distribution of v-V_2O_5. Small variations of the bond valencies (bond lengths) as well as few longer distances ($r_{VO} > 0.22$ nm) do not change the main features of this model.

The effects of metal oxide additions are modelled similar to that of the phosphate glasses so that, in accordance with the observations of $N_{VO} = \sim 4.0$ for $x = 0.5$, metavanadate glasses are formed of chains of two-fold corner-connected VO_4. These VO_4 possess distortions similar to those of the VO_4 suggested for v-V_2O_5. Two VO_4 chain groups replace a pair of VO_5 and VO_4 of v-V_2O_5 for each entity MO that is added. The

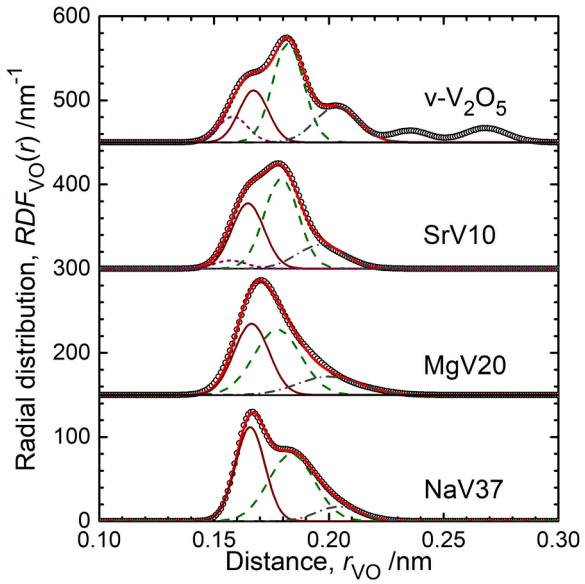

Fig. 7. The V-O first-neighbor distances of vitreous V_2O_5 [21] and of three modified vanadate glasses ([22], this work) calculated from their fit parameters by means of the radial distributions (open circles). Three or four Gaussian functions are adjusted to fit the distributions where the fractions of distances (Fig. 8) follow the simple structural model. The Gaussians represent: V=O double bond ~0.158 nm (short dashed line), other overbonded V-O of ~0.166 nm (solid line), single V–O bonds with lengths of ~0.180 nm (dashed lines), underbonded V-*O* >0.190 nm (dash-dotted line).

terminal V-O (bond length 0.166 nm) of the chain groups coordinate the metal cations. There are three types of V-O bonds in the simple model ($V\text{-}O_{short}$ ~0.166 nm; $V\text{-}O_{middle}$ ~0.180 nm; $V\text{-}O_{long}$ ~0.20 nm). The corresponding numbers N_i of bonds per V atom are calculated with

$$N_s = \frac{(3-2x)}{2(1-x)},\quad N_m = 2 \quad \text{and} \quad N_l = \frac{(1-2x)}{(1-x)} \tag{2}$$

and their sum is N_{VO}. Here, x is the metal oxide content. The fraction N_s includes the very short V=O bonds of ~0.156 nm. These short bonds are shown in Fig. 7 as separate peak for v-V_2O_5 and partially for SrV10. It is assumed that the V=O of a VO_5 participate in the M-O coordination which elongates this bond to ~0.166 nm (two V=O for each M^{2+}). The evolution of the N_i numbers (Eq. (2)) is shown in Fig. 8 where it is compared with the behavior of the phosphate glasses with two types of P-O bonds [27]. The total N_{VO}'s of the model agree with the behavior of the mean values of experimental N_{VO} that are given in Fig. 4. Fig. 7 shows the corresponding modelling of the distributions of the V-O bonds for the glasses SrV10 and MgV20. A fit with only two types of V-O bonds according to the fractions $P\text{-}O_T$ and $P\text{-}O_B$ of phosphate glasses (Fig. 8) was not successful for these samples. modelling of the V-O distances of the NaV37 glass is satisfactory, as well. Since this glass has a composition close to the metavanadate one, also the fit with two types of V-O bonds according the fractions of $P\text{-}O_T$ and $P\text{-}O_B$ bonds was successful.

The VO_5 square pyramid was already discussed as a structural unit of the $(V_2O_5)_{0.5}(P_2O_5)_{0.5}$ glass (chapter 4.2), which is also in accordance with the SOJT effects. The four corners of the pyramidal base can form four equivalent bonds with the isolated PO_4 units. That stabilizes the displacement of the V^{5+} to a corner of the VO_6 (forming a V=O bond). A work on $(V_2O_5)_{0.33}(TeO_2)_{0.67}$ glass [25] reports dominating TeO_3 trigonal pyramids together with VO_5 and VO_6 units. Due to limited resolving power their detailed distances cannot be discussed. The $(V_2O_5)_x(TeO_2)_{1-x}$ glasses of $0.04 \le x \le 0.25$ studied by diffraction of better real-space resolution was aimed at analyzing the TeO_n units [61]. Short V-O bonds of ~0.165 nm are clearly visible. The other V-O distances overlap with the Te-O distances. Due to the larger number of Te

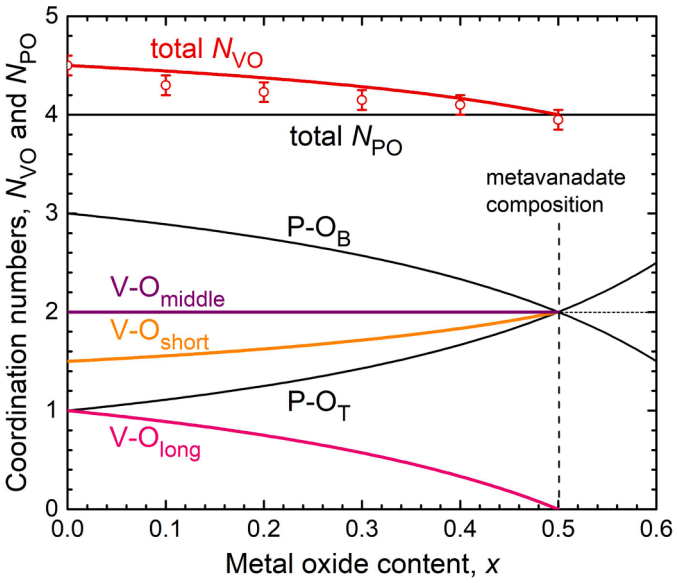

Fig. 8. Behavior of the mean numbers of V-O bonds of three distances according to the typical groups of the simple structural model. The fractions of the VO_5 square pyramid and the VO_4 tetrahedron change with the metal oxide content and, accordingly, the fractions of bond lengths. The total N_{VO} is compared with the mean values of V-O coordination numbers from Fig. 4. The total N_{PO} of modified phosphate glasses is constant four where the fractions of short P-O_T and long P-O_B bonds change with the metal oxide content.

atoms together with their two times stronger X-ray scattering a certain determination of the character of the distorted VO_n units was not possible.

Some recent work investigates structure and properties of multi-component vanadate glasses, for example, Li_2O-V_2O_5-P_2O_5-Fe_2O_3 glasses as cathode material for rechargeable batteries [62] or V_2O_5-P_2O_5-Fe_2O_3 glasses of good water durability [63]. Clarification of the VO_n units by HEXRD would be difficult. EXAFS could help because it yields the environments of selected elements. The authors [62,63] have used V K-edge EXAFS but the corresponding Fourier transforms are only qualitatively discussed. A thorough analysis of the EXAFS data is difficult in the case of several prominent bond lengths, i.e. in the case of strongly deformed structural groups. A straightforward analysis such as known for the pair distributions from HEXRD is not possible.

5. Conclusions

The description of the structure of the binary vanadate glasses always suffered from the poor understanding of the structure of glassy V_2O_5. According to the increase of the V-O coordination number from ~4.0 for $(MO)_{0.5}(V_2O_5)_{0.5}$ glasses to ~4.5 for vitreous V_2O_5 a structure between that of vitreous P_2O_5 and that of the V_2O_5 crystal must be expected. Thus, a structure between three-fold corner-connected VO_4 tetrahedra and edge-connected VO_5 square pyramids should exist. On the other hand, the structure of the $(V_2O_5)_{0.5}(P_2O_5)_{0.5}$ glass is obviously formed of the same building blocks as its crystalline counterpart $VOPO_4$, thus, with dominantly corner-connected VO_5 square pyramids.

The latter crystal shows features that are important for the formation of a glass: It is free of three-fold coordinated oxygen and there are no edge-connected groups. One could simply replace the four-fold corner-connected PO_4 by VO_4 to obtain a V_2O_5 structure because that would satisfy the coordination number 4.5. However, that would not satisfy that distribution of V-O distances of v-V_2O_5 which was obtained by HEXRD. Previous reverse Monte-Carlo simulations of v-V_2O_5 satisfied both N_{VO} = 4.5 and the distribution of V-O distances from HEXRD. Unfortunately, the diverse VO_n groups did not meet the requirements of balanced bond valences sufficiently.

At this point it was remembered the SOJT effects which explain the formation of distorted VO_6 groups of numerous crystalline vanadates, among them in V_2O_5 and $VOPO_4$. VO_5 square pyramids (one short, four longer bonds) and distorted VO_4 (two short and two longer bonds) result from the common out-of-center displacements of the V^{5+} in VO_6 octahedra. Finally, the disordered network of these groups produces the experimental length distribution of V-O bonds of v-V_2O_5. The VO_4 chain groups are formed if modifier oxide MO is added. These VO_4 have the same distortion as those suggested for the network of v-V_2O_5 but the oxygens in their short V-O bonds are terminal and coordinate the modifier ions. Now, a satisfactory fit of the distributions of the V-O distances from HEXRD of the binary vanadate glasses of small modifier content was possible.

The use of HEXRD was revealed to be very useful because distance distributions of the V-O bonds with two or three prominent distances help to identify the structural groups. The use of a large collection of samples measured with HEXRD increases the certainty of the results.

Author contributions

U. Hoppe: Conceptualization, Diffraction experiments, Formal analysis, Writing – original draft. A. Ghosh: Conceptualization, Funding acquisition, Preparation of samples. S. Feller: Conceptualization, Funding acquisition, Preparation of samples, Writing – editing. A. C. Hannon: Neutron diffraction. D. A. Keen: Neutron diffraction. J. Neuefeind: X-ray diffraction.

Declaration of Competing Interest

The authors declare that they have no known competing financial interests or personal relationships that could have appeared to influence the work reported in this paper.

Acknowledgements

The National Science Foundation of the United States is thanked under grant number NSF-DMR 1746230. The Science and Engineering Research Board of India is also thanked for the J C Bose National Fellowship grant number SB/S2/JCB-33/2014.

References

[1] W. Vogel, Glass Chemistry, 3rd Ed., Springer-Verlag New York, Berlin, Heidelberg, 1992.
[2] Y. Sakurai, J. Yamaki, Correlation between microstructure and electrochemical behavior of amorphous V_2O_5-P_2O_5 in lithium cells, J. Electrochem. Soc. 135 (1988) 791–796.
[3] G. Silversmit, J.A. van Bokhoven, H. Poelman, A.M.J. van der Eerden, G.B. Marin, M.-F. Reyniers, R.D. Gryse, The structure of supported and unsupported vanadium oxide under calcination, reduction and oxidation determined with XAS, Appl. Cat. A Gen. 285 (2005) 151–162.
[4] U. Hoppe, R. Kranold, E. Gattef, J. Neuefeind, D.A. Keen, An X-ray and neutron scattering study of the structure of zinc vanadate glasses, Z. Naturforsch. 56a (2001) 478–488.
[5] T. Aoyagi, S. Kohara, T. Naito, Y. Onodera, M. Kodama, T. Onodera, D. Takamatsu, S. Tahara, O. Saketa, T. Miyake, K. Suzuya, K. Ohara, T. Usuki, Y. Hayashi, H. Takizawa, Controlling oxygen coordination and valence of network forming cations, Sci. Rep. 10 (2020) 7178 (11).
[6] R. Enjalbert, J. Galy, A refinement of the structure of V_2O_5, Acta Cryst. C 42 (1986) 1467–1469.
[7] U. Hoppe, G. Walter, A. Barz, D. Stachel, A.C. Hannon, The P-O bond lengths in vitreous P_2O_5 probed by neutron diffraction with high real-space resolution, J. Phys.: Condens. Matter 10 (1998) 261–270.
[8] D.W.J. Cruickshank, Refinements of structures containing bonds between Si, P, S or Cl and O or N. VI. P_2O_5, form III, Acta Cryst 17 (1964) 679–680.
[9] A. Magnus, Über chemische Komplexverbindungen, Z. anorg. Chem. 124 (1922) 289–321.
[10] V.M. Goldschmidt, Geochemische Verteilungsgesetze der Elemente, Skr. Nor. Vidensk. Oslo I 8 (1926) 69.
[11] R.D. Shannon, C.T. Prewitt, Effective ionic radii in oxides and fluorides, Acta Cryst. B 29 (1969) 925.

[12] R.D. Shannon, Revised effective ionic radii and systematic study of inter atomic distances in halides and chalcogenides, Acta Cryst. A 32 (1976) 751–767.
[13] D.W. Cruickshank, 1077. The rôle of 3d-orbitals in π-bonds between (a) silicon, phosphorus, sulphur, or chlorine and (b) oxygen or nitrogen, J. Chem. Soc. (1961) 5486–5504.
[14] R. Gopal, C. Calvo, Crystal structure of β-VPO_5, J. Solid State Chem. 5 (1972) 432–435.
[15] U. Öpik, M.H.L. Pryce, Studies of the Jahn-Teller effect I. A survey of the static problem, Proc. R. Soc. Lond. A 238 (1957) 425–447.
[16] R.G. Pearson, Concerning Jahn-Teller Effects, Proc. Nat. Acad. Sci. 72 (1975) 2104–2106.
[17] R.A. Wheeler, M.-.H. Whangbo, T. Hughbanks, R. Hoffmann, J.K. Burdett, T. A. Albright, Symmetry vs. Asymmetric linear M-X-M linkages in molecules, polymers, and extended networks, J. Am. Chem. Soc. 108 (1986) 2222–2236.
[18] M. Kunz, I.D. Brown, Out-of-center distortions around octahedrally coordinated d^0 transition metals, J. Solid State Chem. 115 (1995) 395–406.
[19] U. Hoppe, E. Yousef, C. Rüssel, J. Neuefeind, A.C. Hannon, Structure of vanadium tellurite glasses studied by neutron and X-ray diffraction, Solid State Comm. 123 (2002) 273–278.
[20] U. Hoppe, R. Kranold, J.M. Lewis, C.P. OBrien, H. Feller, S. Feller, M. Affatigato, J. Neuefeind, A.C. Hannon, Structure of binary alkaline earth vanadate glasses: an x-ray and neutron diffraction investigation, Phys. Chem. Glasses 44 (2003) 272–279.
[21] U. Hoppe, N.P. Wyckoff, M.L. Schmitt, R.K. Brow, A. Schöps, A.C. Hannon, Structure of V_2O_5-P_2O_5 glasses by X-ray and neutron diffraction, J. Non-Cryst. Solids 358 (2012) 328–336.
[22] U. Hoppe, R. Kranold, A. Ghosh, J. Neuefeind, D.T. Bowron, X-ray and neutron scattering studies of the structure of strontium vanadate glasses, Phys. Chem. Glasses: Eur. J. Glass Sci. Technol. B 61 (2020) 200–205.
[23] H. Munemura, S. Tanaka, K.K. Maruyama, M. Misawa, Structural study of Li_2O-V_2O_5 glasses by neutron and X-ray diffraction, J. Non-Cryst. Solids 312-314 (2002) 557–560.
[24] U. Hoppe, R. Kranold, A. Ghosh, C. Landron, J. Neuefeind, P. Jóvári, Environments of lead cations in oxide glasses probed by X-ray diffraction, J. Non-Cryst. Solids 328 (2003) 146–156.
[25] P. Rozier, A. Burian, G.J. Cuello, Neutron and X-ray scattering studies of Li_2O-TeO_2-V_2O_5 glasses, J. Non-Cryst. Solids 351 (2005) 632–639.
[26] K. Suzuki, M. Ueno, Experimental Discrimination between bridging and nonbridging Oxygen – Phosphorus bonds in P_2O_5-Na_2O Glass by Pulsed Neutron Total Scattering, J. de Physique 46 (1985) 261–265. C8.
[27] U. Hoppe, G. Walter, R. Kranold, D. Stachel, Structural specifics of phosphate glasses probed by diffraction methods: a review, J. Non-Cryst. Solids 263 (2000) 29–47.
[28] S. Sen, A. Ghosh, Structure and other physical properties of magnesium vanadate glasses, J. Non-Cryst. Solids 258 (1999) 29–33.
[29] J.M. Lewis, C.P. OBrien, M. Affatigato, S.A. Feller, Physical properties of alkali and mixed lithium-cesium vanadate glasses prepared over an extended range of compositions, J. Non-Cryst. Solids 293-295 (2001) 663–668.
[30] D. Waasmaier, A. Kirfel, New analytical scattering-factor functions for free atoms and ions, Acta Cryst. A 51 (1995) 416–431.
[31] E.N. Maslen, A.G. Fox, M.A. O'Kiefe, International Tables for Crystallography, vol. C, in: A. J. C. Wilson (Ed.) Kluwer Academic, Dordrecht, 1992, p. 476.
[32] J.H. Hubbell, Wm.J. Veigele, E.A. Briggs, R.T. Brown, D.T. Cromer, R.J. Howerton, Atomic form factors, incoherent scattering functions, and photon scattering cross sections, J. Phys. Chem. Ref. Data 4 (1975) 471–538.
[33] T.E. Faber, J.M. Ziman, A theory of electrical properties of liquid metals, Philos. Mag. 11 (1965) 153–173.
[34] Y. Waseda, The Structure of Non-Crystalline Materials, McGraw-Hill, New York, 1980, p. 11.
[35] A.C. Hannon, W.S. Howells, A.C. Soper, IOP Conf. Series 107 (1990) 193.
[36] E.A. Lorch, Neutron diffraction by Germania, silica and radiation-damaged silica glasses, J. Phys. C 2 (1969) 229–237.
[37] R.L. Mozzi, B.E. Warren, The structure of vitreous silica, J. Appl. Cryst. 2 (1969) 164–172.
[38] A.J. Leadbetter, A.C. Wright, Diffraction studies of glass structure: I. Theory and quasi-crystalline model, J. Non-Cryst. Solids 7 (1972) 23–36.
[39] A.C. Hannon, Neutron diffraction techniques for structural studies of glasses, in: M. Affatigato (Ed.), Modern Glass Characterization, John Wiley & Sons, Hoboken, New Jersey, 2015 p 190ff.
[40] O.B. Lapina, D.F. Khabibulin, A.A. Shubin, V.V. Terskikh, Practical aspects of ^{51}V and ^{93}Nb solid-state NMR spectroscopy and applications to oxide materials, Prog. Nucl. Mag. Res. Spec. 53 (2008) 128–191.
[41] S. Hayakawa, T. Yoko, S. Sakka, Structural Studies on Alkaline Earth Vanadate Glasses (Part 2) ^{51}V NMR Spectroscopy Study, J. Ceram. Soc. Japan 102 (1994) 530–536.
[42] R. Gopal, C. Calvo, Crystal structure of β-VPO_5, J. Solid State Chem. 5 (1972) 432–435.
[43] P.T. Nguyen, R.D. Hoffman, A.W. Sleight, Structure of $(VO)_2P_2O_7$, Mat. Res. Bull. 30 (1995) 1055–1063.
[44] S. Stizza, I. Davoli, O. Gzowski, L. Murawski, M. Tomellini, A. Marcelli, A. Bianconi, EXAFS and XANES joint analyses for semiconducting vanadium phosphate glasses, J. Non-Cryst. Solids 80 (1986) 175–180.
[45] W.H. Zachariasen, The atomic arrangement in glass, J. Am. Ceram. Soc. 54 (1932) 3841–3851.
[46] H. Morikawa, M. Miyake, S. Iwai, K. Furukawa, A. Revcolevschi, Structural analysis of molten V_2O_5, J. Chem. Soc. Faraday Trans. I 77 (1981) 361–367.
[47] G.D. Andreetti, G. Calestani, A. Montenero, M. Bettinelli, Refinement of the crystal structure of ZnV_2O_6, Z. Kristallogr. 168 (1984) 53–58.
[48] H.N. Ng, C. Calvo, Crystal structure of and electron spin resonance of Mn^{2+} in MgV_2O_6, Can. J. Chem. 50 (1972) 3619–3624.
[49] J.C. Bouloux, G. Perez, J. Galy, Structure crystalline des metavanadates CaV_2O_6 et CdV_2O_6 alpha, Bull. Soc. Franc. Mineral. Crist. 95 (1972) 130–133.
[50] M.A. Simonov, O.G. Karpov, T.I. Krasnenko, O.A. Sabara, Crystal structure of α-SrV_2O_6, Kristallografiya 34 (1989) 1392–1395.
[51] F. Marumo, M. Isobe, S.I. Iwai, Y. Kondo, α-Form of Sodium Metavanadate, Acta Cryst. B 30 (1974) 1628–1630.
[52] F.C. Hawthorn, C. Calvo, The crystal chemistry of the M^+VO_3 (M+ = Li, Na, K, NH_4, Tl, Rb, and Cs) pyroxenes, J. Solid State Chem. 22 (1977) 157–170.
[53] A.D. Wadsley, Crystal chemistry of non-stoichiometric pentavalent vanadium oxides: crystal structure of $Li_{1+x}V_3O_8$, Acta Cryst 10 (1957) 261–267.
[54] U. Hoppe, R. Kranold, E. Gattef, An X-ray diffraction study of the structure of vitreous V_2O_5, Solid State Commun 108 (1998) 71–76.
[55] U. Hoppe, R. Kranold, A reverse Monte Carlo study of the structure of vitreous V_2O_5, Solid State Commun 109 (1999) 625–630.
[56] I.D. Brown, The Chemical Bond in Inorganic Chemistry: The Bond Valence Model, University Press, Oxford, 2002.
[57] R.D. Shannon, C. Calvo, Refinement of the refinement crystal structure of low temperature Li_3VO_4 and analysis of mean bond lengths in phosphates, arsenates, and vanadates, J. Solid State Chem. 6 (1973) 538–549.
[58] I.D. Brown, D. Altermatt, Bond-valence parameters obtained from a systematic analysis of the inorganic crystal structure database, Acta Cryst. B 41 (1985) 244–247.
[59] K.M. Ok, P.S. Halasyamani, D. Casanova, M. Llunell, P. Alemany, S. Alvarez, Distortions in octahedrally coordinated d^0 transitional metal oxides: a continuous symmetry measures approach, Chem. Mater. 18 (2006) 3176–3183.
[60] P.S. Halasyamani, Asymmetric cation coordination in oxide materials: influence of lone-pair cations on the intra-octahedral distortion in d^0 transition metals, Chem. Mater. 16 (2004) 3586–3592.
[61] U. Hoppe, E. Yousef, C. Rüssel, J. Neuefeind, A.C. Hannon, Structure of vanadium tellurite glasses studied by neutron and X-ray diffraction, Solid State Commun 123 (2002) 273–278.
[62] T. Aoyagi, T. Fujieda, T. Toyama, K. Kono, D. Takamatsu, T. Hirano, T. Naito, Y. Hayashi, H. Takizawa, Electrochemical properties and in-situ XAFS observation of Li_2O-V_2O_5-P_2O_5-Fe_2O_3 quaternary-glass and crystallized-glass cathodes, J. Non-Cryst. Solids 453 (2016) 28–35.
[63] T. Aoyagi, D. Takamatsu, Y. Onodera, T. Naito, T. Onodera, T. Miyake, S. Kohara, T. Ina, Y. Hayashi, H. Takizawa, Vanadium coordination environment in phospho-vanadate glass for improving water durability, J. Ceram. Soc. Japan 128 (2020) 273–278.